Recruitment of classical monocytes can be inhibited by disturbing heteromers of neutrophil HNP1 and platelet CCL5

Jean-Eric Alard,[1]* Almudena Ortega-Gomez,[1]* Kanin Wichapong,[2] Dario Bongiovanni,[3] Michael Horckmans,[1] Remco T. A. Megens,[1,2] Giovanna Leoni,[1] Bartolo Ferraro,[1,4] Jan Rossaint,[5] Nicole Paulin,[1] Judy Ng,[3] Hans Ippel,[2] Dennis Suylen,[2] Rabea Hinkel,[1,3,6] Xavier Blanchet,[1] Fanny Gaillard,[7] Michele D'Amico,[4] Phillipp von Hundelshausen,[1] Alexander Zarbock,[5] Christoph Scheiermann,[8] Tilman M. Hackeng,[2] Sabine Steffens,[1,6] Christian Kupatt,[3,6] Gerry A. F. Nicolaes,[2†] Christian Weber,[1,2,6†] Oliver Soehnlein[1,6,9‡]

In acute and chronic inflammation, neutrophils and platelets, both of which promote monocyte recruitment, are often activated simultaneously. We investigated how secretory products of neutrophils and platelets synergize to enhance the recruitment of monocytes. We found that neutrophil-borne human neutrophil peptide 1 (HNP1, α-defensin) and platelet-derived CCL5 form heteromers. These heteromers stimulate monocyte adhesion through CCR5 ligation. We further determined structural features of HNP1-CCL5 heteromers and designed a stable peptide that could disturb proinflammatory HNP1-CCL5 interactions. This peptide attenuated monocyte and macrophage recruitment in a mouse model of myocardial infarction. These results establish the in vivo relevance of heteromers formed between proteins released from neutrophils and platelets and show the potential of targeting heteromer formation to resolve acute or chronic inflammation.

INTRODUCTION

The sequence of phagocyte recruitment to the site of inflammation comprises an initial extravasation of neutrophils followed by a subsequent emigration of monocytes. That this sequence is not a coincidence but that neutrophils indeed generate signals that recruit monocytes stems from animal models of induced neutropenia (*1*–*4*). Several mechanisms that contribute to the transition from neutrophil to monocyte recruitment have been identified, wherein the release of chemotactic granule proteins is of specific importance (*5*). Lysates of neutrophils exert chemotactic activity on monocytes, suggesting an important role for preformed stores of cellular mediators in launching monocyte extravasation (*6*). Further support for such causal connection stems from patients with functional neutrophil deficits. Neutrophil lysates of patients suffering from specific granule deficiency lack their chemotactic effect on monocytes (*7*). Neutrophils from these patients are devoid of granule proteins such as human neutrophil peptides (HNPs; α-defensins) and human cationic antimicrobial protein 18 (proform of LL-37) (*8*). Subsequently neutrophil-borne, LL-37, azurocidin, cathepsin G, and HNP1 to HNP3 (α-defensins) were demonstrated to be chemotactic for human and murine monocytes (*3*, *9*, *10*).

Similarly to neutrophils, platelets have been implicated in monocyte recruitment (*11*). Recent proteomic analyses revealed the abundance of classical chemokines in platelet α and dense granules (*12*). Deposition of CXCL4 on the endothelium by activated platelets results in subsequent monocyte adhesion (*13*). Other abundant chemokines in platelet granules are CXCR2 ligands such as CXCL7, MIF, CXCL3, CXCL2, and CXCL5 that mediate monocyte activation and adhesion (*14*, *15*). Finally, platelets store CCL5, a potent chemokine for monocytes and lymphocytes alike (*16*).

The existence of distinct monocyte subsets has been established in human and mouse blood (*17*, *18*). Whereas classical monocytes ($CD14^{+}CD16^{-}$ in humans and $Ly6C^{hi}CCR2^{+}CD62L^{+}CX_3CR1^{mid}$ in mice) are rapidly recruited to sites of injury and differentiate into inflammatory macrophages after extravasation (*19*), nonclassical monocytes ($CD14^{low}CD16^{+}$ in humans and $Ly6C^{low}CCR2^{-}CD62L^{-}CX_3CR1^{hi}$ in mice) patrol the vascular lumen (*20*). Monocyte recruitment and activation have been shown to be detrimental in acute and chronic inflammation, including myocardial infarction, atherosclerosis, sepsis, and acute lung injury (*21*, *22*). In these pathologies, recruitment of monocytes is accompanied by systemic activation of neutrophils and platelets, thus allowing for cooperation of both cell types in monocyte recruitment. Given the importance of neutrophil and platelet secretory products during monocyte recruitment, we here aimed at dissecting how neutrophil and platelet granule proteins join forces to enhance tissue monocyte infiltration. We identify a crucial importance of protein heteromers formed between neutrophil-derived HNP1 and platelet-borne CCL5. On this basis, we designed a small peptide that could disturb the interaction between HNP1 and CCL5 and prevent monocyte recruitment in basic inflammation models as well as a mouse model of myocardial infarction.

RESULTS

Neutrophil and platelet secretory products cooperate in adhesion of classical monocytes

To study the cooperation of neutrophil and platelet secretory products in monocyte adhesion, we deposited the supernatant from activated neutrophils (PMN_{sup}) and platelets (Plt_{sup}) on human umbilical vein

[1]Institute for Cardiovascular Prevention, Ludwig Maximilians University Munich, 80336 Munich, Germany. [2]Department of Biochemistry, Cardiovascular Research Institute Maastricht, University Maastricht, 6200 Maastricht, Netherlands. [3]Medizinische Klinik I, Technische Universität München, 81675 Munich, Germany. [4]Department of Experimental Medicine, University of Naples, 80138 Naples, Italy. [5]Department of Anesthesiology, University of Münster, 48149 Münster, Germany. [6]German Centre for Cardiovascular Research, partner site Munich Heart Alliance, 80336 Munich, Germany. [7]Roscoff Biological Station, Pierre et Marie Curie University, 29682 Paris, France. [8]Walter-Brendel-Center of Experimental Medicine, Ludwig Maximilians University Munich, 81377 Munich, Germany. [9]Department of Pathology, Academic Medical Center, 1105 Amsterdam, Netherlands.
*These authors contributed equally to this work.
†These authors contributed equally to this work.
‡Corresponding author. E-mail: oliver.soehnlein@gmail.com

endothelial cells (HUVECs) alone or in combination (PMN/Plt_{sup}). Although monocyte adhesion was not affected in the presence of PMN_{sup} or Plt_{sup}, PMN/Plt_{sup} enhanced arrest of classical but not nonclassical monocytes (Fig. 1, A to C) to a similar degree to that observed after endothelial cytokine activation (fig. S1A). Deposition of PMN/Plt_{sup} evoked similar effects on classical monocyte adhesion when HUVECs were preactivated with tumor necrosis factor (TNF) (Fig. 1D). To assess the in vivo relevance of these findings, we studied monocyte adhesion to postcapillary venules in the cremaster muscle of *$Cx_3cr1^{egfp/wt}$* mice (*23*). Adhesion of monocyte subsets was tested after trauma-induced activation (Fig. 1, E and F, and fig. S1B) or by intrascrotal TNF activation (Fig. 1, G to L). In accordance with observations made in vitro, intravenous injection of PMN_{sup} or Plt_{sup} alone did not affect adhesion or rolling of either monocyte subset, whereas administration of PMN/Plt_{sup} induced a shift from the fraction of rolling classical monocytes toward the adherent fraction (Fig. 1, H to J). In contrast, rolling and adhesion of nonclassical monocytes were not affected (Fig. 1, K and L).

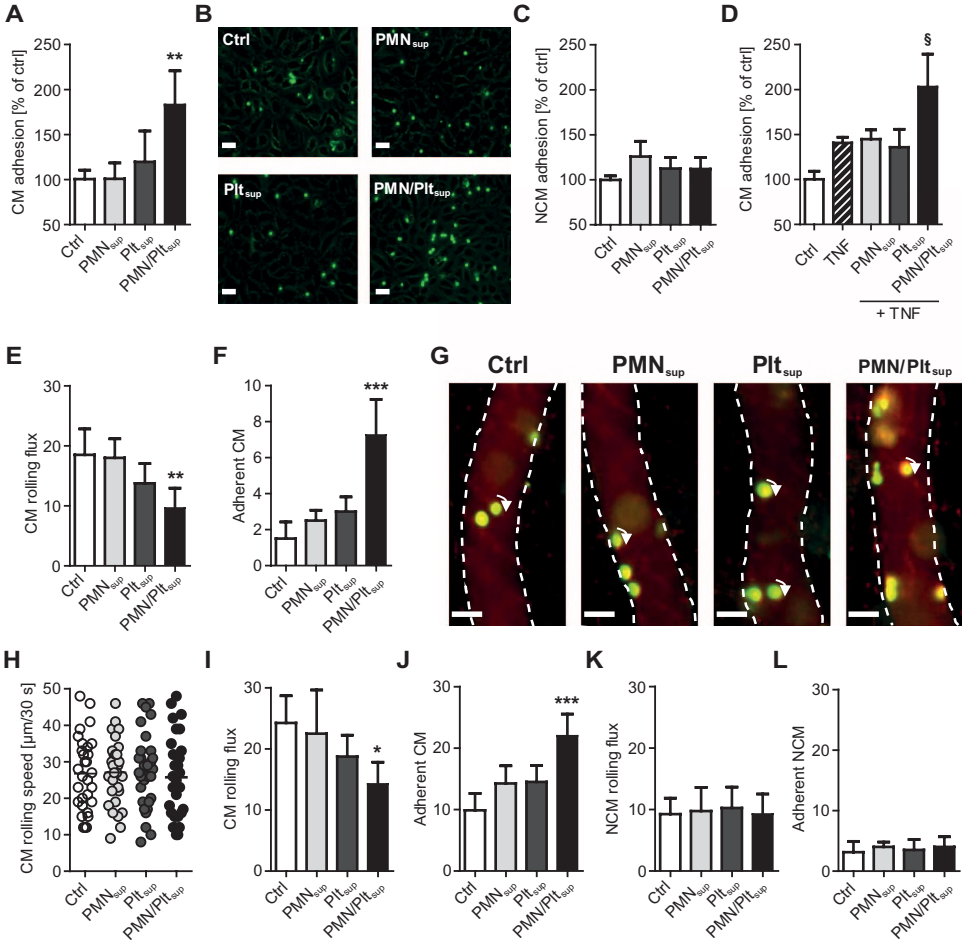

Fig. 1. Neutrophil and platelet secretory products enhance adhesion of classical monocytes. (**A** to **D**) Human classical (A, B, and D) or nonclassical (C) monocytes were perfused over resting (A to C) or TNF-activated (D) (50 ng, 12 hours) HUVEC monolayers, and the number of adherent cells was quantified. Neutrophil supernatant (PMN_{sup}), platelet supernatant (Plt_{sup}), or a combination of both (PMN/Plt_{sup}) was deposited 5 min before perfusion. Green cells in (B) represent calcein-labeled classical monocytes. (**E** to **L**) Intravital epifluorescence microscopy of acutely exposed cremaster muscles (E and F) or TNF-activated cremaster muscles (G to L) in *$Cx_3cr1^{egfp/WT}$* mice. To discriminate between monocyte subsets, a phycoerythrin (PE)–conjugated antibody to Ly6C (1 µg) was introduced intravenously. PMN_{sup}, Plt_{sup} (100 µl), or a combination of both was injected 15 min before recording. Rolling speed (H), rolling flux (E, I, and K), and adhesion (F, J, and L) of classical monocytes (CM) (E, F, and H to J) or nonclassical monocytes (NCM) (K and L) were quantified. (G) Representative images: classical monocytes in yellow and nonclassical monocytes in green. Scale bars, 20 µm. Rolling speed is measured in 5 cells per cremaster muscle. Kruskal-Wallis with Dunn's posttest, $^*P < 0.05$, $^{**}P < 0.01$, $^{***}P < 0.001$ versus ctrl, $^{§}P < 0.05$ versus TNF; $n = 6$.

Platelet CCL5 and neutrophil HNP1 liaise to stimulate monocyte adhesion

Chemoattractants released from granules of neutrophils and platelets can be sensed by monocytes through various chemotactic receptors including formyl peptide receptors (FPRs) and chemokine receptors (*5*, *15*). Specific inhibition of FPRs or the chemokine receptors CXCR2 and CCR2 had no effect on PMN/Plt_{sup}-evoked classical monocyte adhesion (Fig. 2A). In contrast, neutralization of CCR5 signaling abrogated stimulated monocyte adhesion. Hence, we suspected that CCL5, a major CCR5 ligand, may be an important factor in this response. In line herewith, PMN/Plt_{sup} depleted of CCL5 was nonfunctional (Fig. 2B). However, when comparing PMN_{sup} and Plt_{sup}, CCL5 is exclusively released from platelets (Fig. 2C). Thus, we assumed that CCL5 may bind a partner within the PMN_{sup} to potentiate its effect. To investigate this possibility, we immunoprecipitated CCL5 from the PMN/Plt_{sup} and assessed CCL5-binding partners by mass spectrometry (table S1). Among the identified proteins were four, which are released from neutrophils and exert a chemotactic response: HNPs, S100A8/A9 (MRP8/14), cathepsin G, and azurocidin. In flow experiments, no neutrophil granule protein enhanced classical monocyte adhesion by itself (Fig. 2D). However, when combined with CCL5, HNPs, but not the other granule proteins, specifically evoked enhancement of classical monocyte adhesion (Fig. 2D). The importance of HNPs and CCL5 was confirmed by depletion of HNPs or HNPs and CCL5, which abrogated monocyte adhesion stimulated by PMN/Plt_{sup} (Fig. 2E). HNPs comprise a group of three proteins that differ in just one amino acid. As HNP1, HNP2, and HNP3 were equally potent in enhancing monocyte adhesion when combined with CCL5 (fig. S2A), we performed further experiments with HNP1, the most abundant α-defensin family member. Because HNP1 in combination with CCL5 strongly enhanced adhesion of human classical monocytes (Fig. 2D and fig. S2B) but not nonclassical monocytes (fig. S2C), we

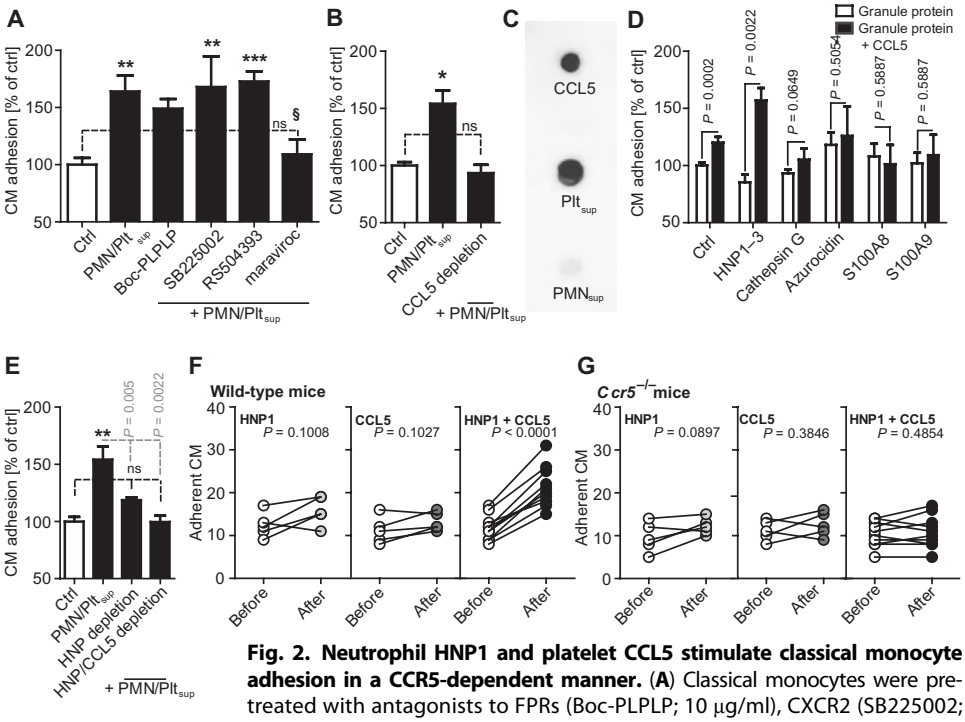

Fig. 2. Neutrophil HNP1 and platelet CCL5 stimulate classical monocyte adhesion in a CCR5-dependent manner. (**A**) Classical monocytes were pretreated with antagonists to FPRs (Boc-PLPLP; 10 μg/ml), CXCR2 (SB225002; 5 μg/ml), CCR2 (RS504393; 1.5 μg/ml), CCR5 (maraviroc; 3 μg/ml), or vehicle control and perfused over HUVECs, where PMN/Plt_{sup} was deposited. Kruskal-Wallis with Dunn's posttest, $^{**}P < 0.01$, $^{***}P < 0.001$ versus ctrl, $^{§}P < 0.05$ versus PMN/Plt_{sup} in Dunn's posttest; $n = 6$. ns, not significant. (**B**) Classical monocytes were perfused over HUVECs, where native or CCL5-depleted PMN/Plt_{sup} was deposited. Kruskal-Wallis with Dunn's posttest, $^{*}P < 0.05$ versus other groups; $n = 6$. (**C**) Representative dot blot with hCCL5, Plt_{sup}, and PMN_{sup} spotted on a membrane, which was probed with a CCL5 antibody. (**D**) Classical monocytes were perfused over HUVECs, where CCL5 (1 μg/ml) alone (ctrl) or in combination with neutrophil-derived chemotactic proteins HNP1 to HNP3, cathepsin G, azurocidin, S100A8, and S100A9 (each 10 μg/ml) were deposited. Mann-Whitney test. $n = 6$ to 8. (**E**) Classical monocytes were perfused over HUVECs, where native PMN/Plt_{sup} or PMN/Plt_{sup} depleted of HNPs or HNPs and CCL5 was deposited. Kruskal-Wallis with Dunn's posttest, $^{**}P < 0.01$ versus ctrl, exact P values assessed by Mann-Whitney test; $n = 6$. (**F** and **G**) Intravital epifluorescence microscopy of TNF-activated cremaster muscles in wild-type (F) or $Ccr5^{-/-}$ (G) mice injected with a PE-conjugated antibody to Ly6C. Cell adhesion was quantified before and 15 min after injection of HNP1 (10 μg), CCL5 (1 μg), or a combination of both. Paired t test.

challenged the in vivo relevance of this finding in monocyte reporter $Cx_3cr1^{egfp/wt}$ mice. With the absence of HNPs in mouse neutrophils (*24*), we administered human CCL5 (hCCL5) and HNP1 intravenously and experienced an increase in adhesion with a concomitant decrease in rolling flux of classical monocytes (Fig. 2F and fig. S2D). This effect was lost in $Ccr5^{-/-}$ mice (Fig. 2G), suggesting that HNP1 and CCL5 act via CCR5.

CCL5 permits HNP1 to engage CCR5

In ligand-binding assays, rhodamine-conjugated HNP1 did not bind to classical monocytes. However, CCL5 permitted HNP1 binding to human classical monocytes in a dose-dependent fashion (fig. S3A). In proximity ligation assays, we could identify that HNP1 was in close proximity to CCR5 only in the presence of CCL5 (Fig. 3A), suggesting that CCL5 permits HNP1 to access CCR5. This notion was supported by experiments where approximation of HNP1 to CCR5 in the presence of CCL5 was abrogated by a CCR5 antagonist (Fig. 3B). The latter was also confirmed when rhodamine-HNP1 was incubated with Chinese hamster ovary (CHO) cells stably transfected with a CCR5–GFP (green fluorescent protein) construct. Here, CCR5 colocalized with HNP1 and, after cross-linking, comigrated in an SDS–polyacrylamide gel (Fig. 3C and fig. S3B). Together, these data suggest that CCL5 enables HNP1 to access CCR5.

HNP1 and CCL5 form stable heteromers

Thus far, our data pointed toward a protein-protein interaction between HNP1 and CCL5, which synergizes to activate monocytes via CCR5. To further study the interaction between HNP1 and CCL5, we performed surface plasmon resonance studies. Biotinylated CCL5 was immobilized on a streptavidin-coated sensor chip, and HNP1 was superfused, resulting in a dose-dependent interaction [dissociation constant (K_d) = 70 nM] (Fig. 4A). In a reverse approach, HNP1 was immobilized and perfused with increasing concentrations of CCL5, and a similar dose-dependent response was identified (K_d = 8.6 nM) (Fig. 4B). To better characterize the interaction between HNP1 and CCL5, we perfused naturally occurring variants of CCL5 from different species over immobilized HNP1 (Fig. 4C). These data were integrated with in silico studies to predict a likely heteromeric complex structure of HNP1 bound to CCL5, which was subsequently used to design a small peptide to disturb the interaction between HNP1 and CCL5. Assuming conservation of the binding mode for the CCL5-HNP1 complex among species, there should be a correlation between calculated binding free energies and experimental binding affinities. The CCL5-HNP1 complex (Fig. 4D) represents a likely heteromeric complex because this conformation exhibited the highest correlation between calculated binding free energies and experimental K_d (fig. S4) values identified among 21 different potential conformations derived from protein-protein docking. After analysis of this proposed structure, we found that residues from β strands 2 and 3 of HNP1 (^{17}RRYGTCIYQGRLWAFCC^{33}) are the key residues that interact with CCL5. On the basis of the β strand 2 of HNP1 and its binding mode with CCL5 (Fig. 4E), we designed a short peptide (RRYGT**SKY**Q, referred to as the SKY peptide) that exhibited the highest experimental potential to disturb the interaction between CCL5 and HNP1 (Fig. 4F).

Disturbance of HNP1-CCL5 interaction inhibits monocyte adhesion

In inflammation, the endothelium presents proteins secreted from neutrophils and platelets to rolling leukocytes (*25*, *26*). Proximity ligation assays clearly showed abundant interactions of HNP1 and CCL5 on the endothelial cell surface (Fig. 5A), an effect abrogated in the presence

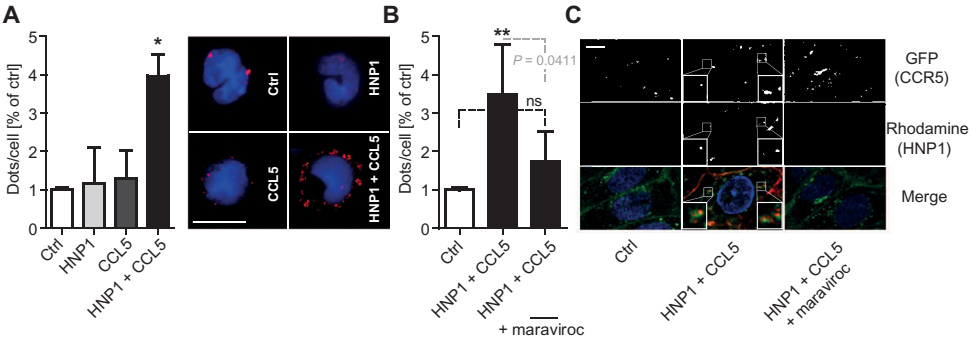

Fig. 3. HNP1 and CCL5 use monocytic CCR5. (**A** and **B**) Proximity ligation assay in human classical monocytes treated with HNP1 (10 μg/ml), CCL5 (1 μg/ml), or a combination of both in the presence (A) or absence (B) of maraviroc (3 μg/ml). Cells were probed with antibodies to CCR5 and HNP1. Kruskal-Wallis with Dunn's posttest, $^{*}P < 0.05$, $^{**}P < 0.01$ versus ctrl, exact *P* values assessed by Mann-Whitney test; $n = 5$ (A) and 6 (B). (**C**) CHO cells stably transfected with a CCR5-GFP construct were incubated with rhodamine-conjugated HNP1 (10 μg/ml) and CCL5 (1 μg/ml) in the presence or absence of maraviroc (3 μg/ml). Colocalization was visualized by confocal microscopy. Boxes represent close-up of sites of co-localization. Scale bar, 5 μm.

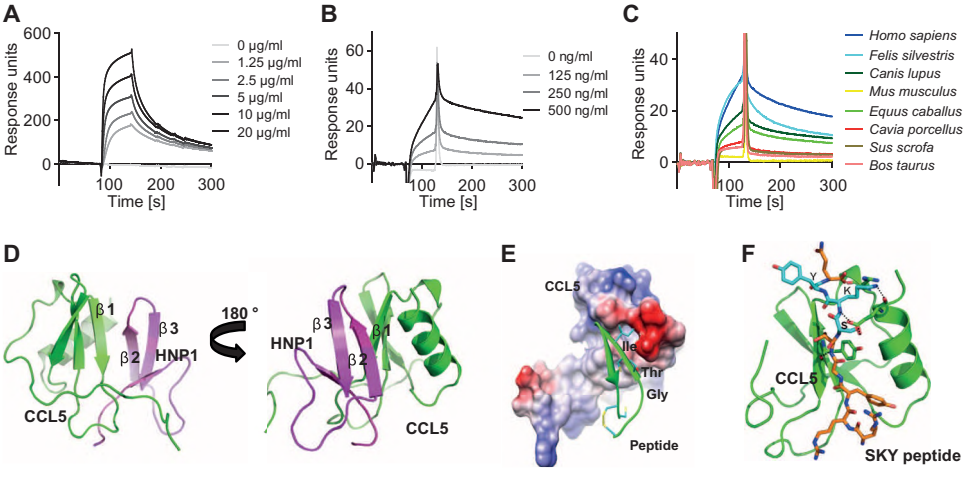

Fig. 4. HNP1 and CCL5 form a targetable heteromer. (**A** to **C**) Surface plasmon resonance reveals interaction between HNP1 and CCL5. Increasing concentrations of HNP1 (A) or CCL5 (B) were perfused over a Biacore sensor chip coated with CCL5 (A) or HNP1 (B). (C) CCL5 from various mammalian species was perfused over an HNP1-coated sensor chip, and the resulting response was assessed. (**D**) Identified heteromer conformation between hCCL5 (green)–HNP1 (magenta) and the interaction between β strand 1 of CCL5 and β strands 2 and 3 of HNP1. (**E**) Template peptide (green ribbon), used as a starting model to design the SKY peptide, projected on the electrostatic molecular surface of CCL5 (red, negative surface; white, neutral surface; and blue, positive surface). Neutral residues such as Gly, Thr, and Ile locate at the negatively charged surface of CCL5. (**F**) Binding mode between CCL5 (green ribbon) and the SKY peptide (RRYGTSKYQ, orange and cyan stick for key residues SKY) that shows interaction with CCL5. H-bond interaction between CCL5 and the SKY peptide is shown in black dashed lines.

of the SKY peptide but not by a scrambled peptide (TYQRRSGKY) (Fig. 5, B and C). These observations were confirmed in vivo in the cremaster muscle after intravenous injection of HNP1 and CCL5 (Fig. 5D). In flow chamber assays, classical monocyte adhesion induced by PMN/Plt_{sup} (Fig. 5E) was abrogated in the presence of the SKY peptide without affecting the viability of the cells involved (fig. S5). In addition, adhesion to coimmobilized HNP1 and CCL5 was dose-dependently reduced by the presence of the SKY peptide (Fig. 5F and fig. S6A). In line with this, intravital microscopy of the cremaster muscle showed that intravenous delivery of the SKY peptide dose-dependently prevented adhesion of classical monocytes induced by coadministration of HNP1 and CCL5 (Fig. 5, G and H, and fig. S6B). To provide an additional control for the specificity of the SKY peptide, we tested its effect on monocyte adhesion in mice not receiving HNP1 and CCL5. In these experiments, the SKY peptide failed to reduce adhesion of classical monocytes (fig. S7, A and B).

To assess the duration of the biological effect after a single dose of the SKY peptide, we first assessed its chemical stability. Using fast protein liquid chromatography, we found that the peptide was stable for the entire observation period of 48 hours (fig. S8A). The biological stability of the effect was tested by intravital microscopy after a single injection of HNP1, CCL5, and the SKY peptide. Monocyte adhesion in the cremaster muscle was recorded for 8 hours after administration of the peptides. HNP1 and CCL5 enhanced monocyte adhesion during the first 6 hours after administration. At 8 hours, no biological effect was observed, likely due to peptide clearance. The SKY peptide abrogated the effects exerted by HNP1-CCL5 immediately after administration, as well as 2, 4, and 6 hours later (fig. S8B). Thus, these data indicate a prolonged inhibitory effect in vivo.

Finally, we aimed at studying the effect of HNP1, CCL5, and the SKY peptide on adhesion of classical monocytes in a different vascular bed. Given the importance of classical monocytes in atherosclerosis (*16*), we decided to study monocyte adhesion in the carotid artery. *Apoe*$^{-/-}$*Cx*$_3$*cr1*$^{egfp/WT}$ mice were fed a high-fat diet for 4 weeks to generate hypercholesterolemia-induced endothelial dysfunction. Adhesion of classical monocytes was studied after injection of a PE-conjugated antibody to Ly6C using established methodology (*16*, *27*). In these experiments, adhesion of classical monocytes was significantly increased by intravenous administration of HNP1 and CCL5, an effect abrogated in the presence of the SKY peptide (fig. S9).

Inhibition of HNP1-CCL5 interaction reduces myocardial macrophage accumulation

Because of the importance of neutrophils and platelets in acute myocardial infarction (*28*), we chose to study adhesion and recruitment of classical monocytes and macrophages 3 days after ischemia-reperfusion of the left anterior descending (LAD) coronary artery. At this time point,

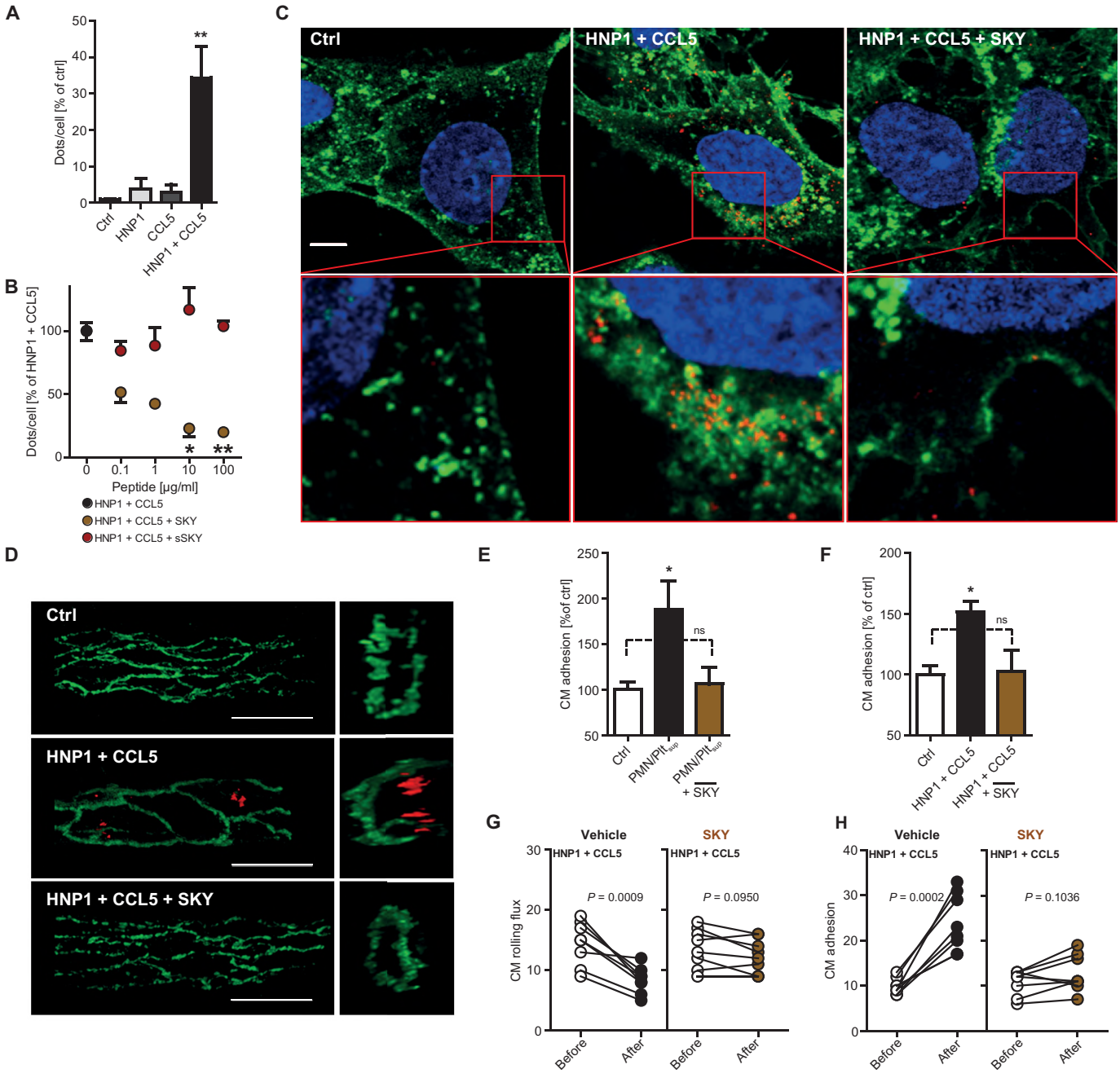

Fig. 5. Disturbance of HNP1-CCL5 interaction abrogates monocyte adhesion evoked by neutrophils and platelets. (**A** to **C**) HNP1 and CCL5 interaction on endothelial cell surfaces can be inhibited by the SKY peptide. Proximity ligation assay on endothelial cells incubated with HNP1 (10 µg/ml), CCL5 (1 µg/ml), or a combination in the absence (A) or presence (B and C) of the SKY peptide or a scrambled peptide (sSKY). Cells were probed with antibodies to HNP1 and CCL5. (C) Representative images of confocal microscopy of untreated, combination of HNP1 and CCL5 in the absence and presence of the SKY peptide (100 µg/ml) on endothelial cell surfaces are displayed. Scale bar, 5 µm. (**D**) The presence of HNP1-CCL5 heteromers in cremasteric venules is abrogated by the SKY peptide. Mice were treated with vehicle (ctrl) or HNP1 (10 µg) and CCL5 (1 µg) in the presence or absence of the SKY (100 µg) peptide. Heteromers were identified by proximity ligation assay (red), and endothelial cells were stained by CD31-directed antibody (green). Extended depth of field projections of cremaster venules (left) and transversal three-dimensional (3D) reconstructions (right) were displayed. Scale bars, 20 µm. (**E** and **F**) The SKY peptide (100 µg/ml) inhibits adhesion of human classical monocytes evoked by immobilized PMN/Plt_{sup} (E) or HNP1/CCL5 (F). Kruskal-Wallis with Dunn's posttest in (A) to (F), *$P < 0.05$, $P < 0.01$ versus ctrl; $n = 5$ (A), 3 (B), 5 (E), and 6 (F). (**G** and **H**) Intravital epifluorescence microscopy of TNF-activated cremaster muscles in $Cx_3cr1^{egfp/WT}$ mice injected with a PE-conjugated antibody to Ly6C. Rolling (G) and adhesion (H) of classical monocytes were quantified before and after HNP1/CCL5 administration in the presence or absence of the SKY peptide (100 µg). Paired *t* test.

neutrophils and platelets can be found in the homogenate of hearts from wild-type mice (fig. S10) and the recruitment of classical monocytes is at its peak (*29*). In these experiments, hCCL5 and HNP1 were overexpressed in the myocardium by adeno-associated virus (AAV)–assisted transduction, reaching plasma levels of 1.7 ± 0.45 μg/ml and 9.13 ± 3.18 μg/ml, respectively. Overexpression in this way resulted in enhanced endothelial adhesion of classical monocytes and accumulation of macrophages in the heart (Fig. 6A), an effect fully abrogated by repetitive treatment with the SKY peptide (Fig. 6B). This effect was only observed in mice with overexpression of hCCL5 and HNP1, but not in wild-type mice, thus strengthening the specificity of the peptide (fig. S7C). Because overexpression of HNP1 and CCL5 and repeated injection of the SKY peptide did neither alter counts of monocytes in the blood nor affect proliferation and apoptosis of monocytes and macrophages in the heart (fig. S11) nor reduce plasma CCL5 (2.00 ± 0.74 μg/ml) and HNP1 levels (6.8 ± 3.5 μg/ml), we conclude that the observed effect on myocardial monocyte and macrophage accumulation primarily stems from alterations of monocyte recruitment. Finally, invasive monitoring of cardiac function revealed that overexpression of hCCL5 and HNP1 resulted in impaired cardiac function. This adverse effect was abolished upon repetitive treatment with the SKY peptide (Fig. 6, C to E).

DISCUSSION

Acute and chronic inflammatory conditions frequently associate with neutrophil and platelet activation. These events represent a causal link to subsequent recruitment of monocytes. Here, we show a novel mechanism of neutrophil-platelet cooperation, which rests upon the heteromer formation of neutrophil HNP1 and platelet CCL5 (movie S1). Both molecules are cationic in nature, thus favoring their immobilization and presentation on vascular endothelium where they can form functional heteromers. These are recognized by monocytes rolling along the endothelium engaging CCR5, thus promoting firm monocyte adhesion. Disturbance of the interaction between HNP1 and CCL5 reduces monocyte adhesion in vitro, in the cremaster muscle, and in a mouse model of myocardial ischemia-reperfusion injury.

The identified paradigm of functional heteromerization of chemotactic molecules released from different cell subsets may offer important therapeutic advantages over direct antagonism or neutralization of chemokines or their receptors. Conclusions toward the effects of a complete blockade of CCL5 in vivo may be inferred from studies in *Ccl5*$^{-/-}$ mice, which show severely impaired polyclonal and antigen-specific T cell proliferation (*30*). Moreover, mice treated with CCR5-targeting Met-RANTES or deficient in CCL5 show delayed viral clearance by macrophages, probably owing to a lack of antiapoptotic signals conferred by CCL5-CCR5 interactions to limit cell-to-cell virus dissemination in the host (*31*, *32*), and Met-RANTES aggravates glomerulonephritis in mice (*33*). In addition, CCL5 was found to be critical in the angiogenic response to ischemia (*34*). Thus, despite the importance of the CCL5-CCR5 axis in atherogenic monocyte recruitment (*16*), direct neutralization of CCL5 may limit healing after myocardial infarction. Similarly, direct interference with HNP1 may impair host defense because HNP1 does not just stand out as a multifunctional immunomodulatory peptide but also as a potent host-derived antimicrobial polypeptide. Consequently, patients lacking HNP1 present with increased susceptibility to pyogenic infections (*8*). Hence, selective disruption of HNP1-CCL5 heteromers, which does not interfere with CCL5-CCR5 interaction, may offer the therapeutic advantage of preserving normal immune defense mechanisms.

CCL5 is recognized by both CCR1 and CCR5 on monocytes. Both receptors have been shown to have specialized roles in leukocyte recruitment (*35*, *36*). Whereas CCR1 was found to be predominantly required for the initial adhesion of monocytes and T cells to endothelial cells, CCR5 appeared to mediate in the first line the spreading on endothelial cells preceding transendothelial migration (*35*). The propensity of CCL5 to form higher-order oligomers has been shown to be particularly important for triggering flow-resistant cell arrest via CCR1, whereas transendothelial migration mediated by CCR5 did not require the oligomerization of CCL5 (*36*). We show that the HNP1-CCL5 heteromer interacts with CCR5 and, as a consequence, makes CCR5 available for mediating monocyte arrest. The

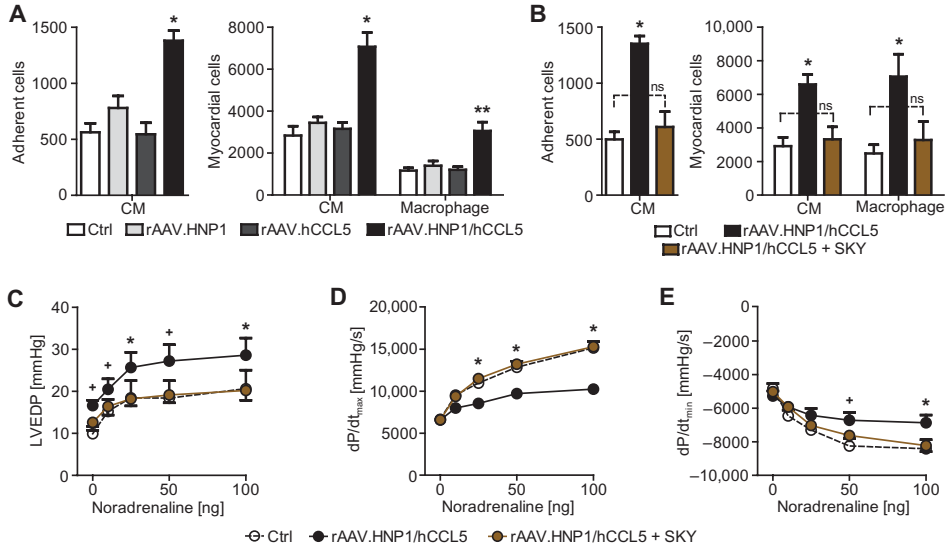

Fig. 6. Disturbance of HNP1-CCL5 interaction reduces myocardial monocyte and macrophage recruitment. (**A**) HNP1 and CCL5 stimulated monocyte recruitment to the myocardium after ischemia-reperfusion. HNP1 and hCCL5 were overexpressed in the myocardium by systemic application of cardiomyotropic AAV2/9 14 days before the ischemic event. Seventy-two hours after myocardial ischemia-reperfusion injury induced by LAD ligation, classical monocytes adherent to the heart vasculature (left panel) and emigrated into the heart (right panels) as well as macrophages in the heart were quantified by flow cytometry. Kruskal-Wallis with Dunn's posttest, $^{*}P < 0.05$, $^{**}P < 0.01$ versus ctrl; $n = 4$. (**B**) The SKY peptide (100 μg every 24 hours) abrogates monocyte recruitment into the heart evoked by HNP1 and hCCL5. Kruskal-Wallis with Dunn's posttest, $^{*}P < 0.05$ versus other groups; $n = 8$. (**C** to **E**) Left ventricular end-diastolic pressure (LVEDP) (C), contraction velocity (dP/dt_{max}) (D), and relaxation velocity (dP/dt_{min}) (E) at baseline and after stimulation with increasing amounts of noradrenaline (10, 25, 50, and 100 ng). Kruskal-Wallis with Dunn's posttest for each dose of noradrenaline, $^{*}P < 0.05$ versus other groups, $^{+}P < 0.05$ versus ctrl; $n = 5$ to 6.

exact structural requirements for this interaction, however, remain to be determined.

Although the ability of HNP1 to exert chemotactic effects has previously been reported, a receptor has so far remained elusive. We show that HNP1 engages CCR5 after heteromerization with CCR5. A similar mechanism has previously been proposed for nonreceptor platelet factor 4, which binds to CCL5 to enhance monocyte adhesion (*37*), and for HMGB1, which exerts its chemotactic effect after heteromerization with CXCL12 (*38*). The unique importance of the HNP1-CCL5 complex resides in the broad relevance of neutrophil and platelet degranulation during various inflammatory conditions including acute arterial occlusion, sepsis, or atherosclerosis. Nevertheless, it is not unlikely that also other chemotactic molecules released from neutrophils and platelets may interact and exert biological activities. Neutrophils carry more than 400 different granule proteins, and platelets store many preformed chemokines, some of which are very promiscuous. Thus, notwithstanding the importance of HNP1-CCL5 heteromers in our study, other heteromers may be relevant in settings not studied here. In addition, the SKY peptide proves effective at higher doses, which can likely not be achieved in a clinical setting. However, the experimental conditions in this study with high concentrations of CCL5 and HNP1 may not reflect a clinical situation where plasma levels of these molecules are typically lower. Thus, to assess the therapeutic feasibility of our concept, additional studies are required. Despite these limitations, our proof-of-principle study indicates that selective interference with the functional interactome constituted by heteromers formed by chemotactic molecules released from different cell types may thereby enable customized treatments of specific inflammatory conditions.

MATERIALS AND METHODS

Study design

The overall objective of this study was to identify the functional cooperativity of soluble mediators released from neutrophils and platelets during the recruitment of monocytes. Subsequent objectives were the identification of mediators involved in this cooperation and the design of an inhibitory strategy. A power analysis for animal experiments was performed using a web-based tool (http://homepage.stat.uiowa.edu/~rlenth/Power/). We assumed a detectable biological difference of at least 50% between up to four groups with an SD of up to 15%, an α of 0.05, and a resultant power of 0.8. On the basis of these assumptions, at least four animals had to be included in each treatment group. The number of biological replicates for each data point is included in the figure legends. All data are included (no outliers were excluded).

Isolation of primary cells and cell culture

Leukocytes were isolated from blood of healthy donors with Polymorphprep density separation (Axis-Shield). Subsequently, classical and nonclassical monocytes were purified from the peripheral blood mononuclear cell fraction with Monocyte Isolation Kit II or $CD16^+$ Monocyte Isolation Kit, respectively (Miltenyi Biotec). Neutrophils were obtained as part of the granulocyte cell fraction. Platelets were isolated from venous blood, collected in anticoagulant citrate dextrose solution (12 mM citric acid, 15 mM sodium citrate, 25 mM glucose, and 3 mM EGTA). Platelet-rich plasma (PRP) was obtained by 5-min centrifugation at 330*g*. To reduce leukocyte contamination, PRP was diluted 1:1 with phosphate-buffered saline (PBS) and centrifuged at 240*g* for 10 min. The supernatant was centrifuged for 15 min at 430*g*, and pelleted platelets were washed once in PBS. Total platelets were counted with a hematology analyzer (XP-300, Sysmex). The purity of neutrophils and platelets was verified by flow cytometry on a FACSCanto II (BD Biosciences) (fig. S12). HUVECs (PromoCell) were cultured on collagen-coated plastic surfaces in endothelial growth medium (PromoCell).

Neutrophil and platelet supernatants

Neutrophil and platelet supernatants were generated with a cell density 20 times higher than the standard average of neutrophil and platelet counts in human blood (150×10^6 platelets/ml and 2.5×10^6 neutrophils/ml). Supernatants were therefore prepared from platelets suspended at 3×10^9/ml and neutrophils suspended at 50×10^6/ml in PBS. To induce activation in platelets, the cell suspension was shaken during 30 min at room temperature, followed by a centrifugation at 16,000*g* to precipitate platelets. Neutrophil degranulation was induced by incubation with fibrinogen-coated Dynabeads M-270 Epoxy (Invitrogen), which was coated according to the manufacturer's instructions. Briefly, batches of 3.3×10^8 beads were coated overnight with 100 μg of fibrinogen (Sigma) at room temperature and subsequently washed with PBS. Neutrophils at 50×10^6/ml were activated with a bead solution at 48×10^8 fibrinogen-coated beads/ml during 1 hour at room temperature. Beads were separated from the neutrophil suspension by magnetic force, and cells were subsequently removed by centrifugation at 300*g* for 5 min. In flow chamber assays, supernatants were used at 1× final concentration in flow adhesion buffer. In in vivo experiments, 1× final concentration was reached by intravenous injection of 100 μl of neutrophil and/or platelet supernatant, assuming a total blood volume per mouse of 1.5 to 2 ml. Immunodepletion of CCL5 and HNP1 in supernatants was performed using magnetic beads (Miltenyi Biotec) conjugated with anti-HNP1 (AbD Serotec) or anti-CCL5 polyclonal antibodies (BD Biosciences). Depletion was confirmed by dot blot analyses using monoclonal antibodies to the respective protein.

Flow chamber assays

HUVECs were grown to confluence and preincubated with neutrophil and/or platelet supernatants or CCL5 (1 μg/ml) and/or HNP1 (10 μg/ml) for 5 min before monocyte perfusion. Freshly isolated monocyte subsets were labeled with green calcein, suspended in flow adhesion buffer (10 mM Hepes, 0.5% bovine serum albumin, 1 mM $MgCl_2$, 1 mM $CaCl_2$), and perfused in a parallel wall flow chamber at a concentration of 1×10^6 monocytes/ml at a shear rate of 1.5 dynes/cm^2. In some experiments, monocytes were pretreated with antagonists to FPRs (Boc-PLPLP; 10 μg/ml), CXCR2 (SB225002; 5 μg/ml), CCR2 (RS504393; 1.5 μg/ml), or CCR5 (maraviroc; 3 μg/ml). The adhesion of monocytes under different conditions was quantified as adherent cells per field of view and calculated as the percentage of the untreated condition (control).

Surface plasmon resonance

Interactions between HNP1 and CCL5 were studied by surface plasmon resonance on a Biacore X100 system (GE Healthcare). Biotinylated CCL5 was immobilized on a streptavidin sensor chip, whereas HNP1 was immobilized on a CM3 chip by amine coupling at a level

of 700 response units. HNP1, HNP2, and HNP3 (Bachem) and CCL5 (PeproTech) were used as analytes and diluted in HBS-EP+. In separate experiments, human chemokines CXCL8, CCL1, CCL3, CCL2, CCL11, CCL17, CX_3CL1 (all PeproTech), human neutrophil proteins cathepsin G, azurocidin (both Athens Research), S100A8, S100A9 (both Prospec), or CCL5 from different species (*Mus* from PeproTech; *Canis* and *Felis* from Creative Biomart; and *Equus*, *Bos*, *Cavia*, and *Sus* from GenWay Biotech Inc.) were used as analytes. Each experiment was performed with a flow of 10 μl/min with running buffer. Sensor chip surfaces were regenerated with 50 mM NaOH and equilibrated with running buffer before the next injection. Results were analyzed with BIAevaluation software.

Protein-protein docking and binding free energy calculations

Sequence alignment between hCCL5 and that of other species (*Bos*, *Canis*, *Cavia*, *Equus*, *Felis*, *Mus*, and *Sus*) revealed a high sequence identity (74 to 88%), which indicates that these CCL5 orthologs are likely to have the same binding mode to HNP1. Potential configurations of hCCL5-HNP1 heteromeric complex were predicted by application of the protein-protein docking protocol implemented in ICM-Pro program. Coordinates of the 3D structures of hCCL5 and HNP1 were obtained from the Protein Data Bank (PDB codes 2L9H and 3HJ2, respectively). Then, homology models for each of the different species of CCL5 were built by using SWISS-MODEL web server and evaluated with WHATCHECK. hCCL5 (2L9H.pdb) was used as a template for the construction of CCL5 models. Next, different model structures for the complex between human HNP1 and the individual CCL5 structures were produced on the basis of conformations of hCCL5 and HNP1 derived from protein-protein docking.

Molecular docking of hCCL5 with human HNP1 yielded 21 different conformations; thus, we obtained a total of 168 different complex structures (21 conformations for each of the eight species included). The derived structures of the CCL5-HNP1 complexes were refined by application of energy minimization and a short molecular dynamics (MD) simulation (100 ps) using Amber12 program, while applying a weak force constraint (10 kcal/mol). Before performing MD simulations, force fields and charges (Amber99SB force field) were assigned to the CCL5-HNP1 complexes. Then, the complex was solvated by water (TIP3P model) and counter ions (Na^+ or Cl^-) within a 9 Å radius. The temperature of the system was set at 300 K. After completion of the MD simulation, snapshots of each complex were extracted for binding free energy calculation using the MM/PBSA approach implemented in Amber12 as described previously (*39*).

Design of small peptide

With the obtained structural information of the likely CCL5-HNP1 heteromeric complex as shown in Fig. 4D, peptides were designed on the basis of the sequence of HNP1 between β strands 2 and 3 (^{17}RRYGTCIYQGRLWAFCC^{33}). This sequence, present at the HNP1 surface that contacts CCL5, was used as a template to design peptides to interfere with the CCL5-HNP1 complex. From the structural analysis, it was concluded that several neutral residues of the wild-type HNP1, such as glycine, threonine, and isoleucine, contact the negatively charged surface of CCL5. Therefore, we modified these residues to positively charged residues to improve the binding affinity with CCL5. Moreover, to avoid potential peptide heteromerization, cysteine at position 22 was modified to serine, which has similar properties but cannot engage in disulfide bonding. The designed peptide was called the SKY peptide (RRYGT**SKY**Q) and is characterized by a calculated binding free energy (−21.90 ± 2.04 kcal/mol), which is considerably lower than that of the original HNP1 sequence (−10.95 ± 1.75 kcal/mol). This implies that the SKY peptide is likely to show high binding affinity with CCL5.

Intravital microscopy

An inflammatory response in $Cx_3cr1^{egfp/wt}$ or $Ccr5^{-/-}$ mice was induced by acute exposure of the cremaster muscle or by intrascrotal injection of TNF (100 ng for 12 hours). The cremaster muscle was exposed, and recordings were made using an Olympus BX51 microscope equipped with a Hamamatsu 9100-02 EMCCD camera (Hamamatsu Photonics), a 40× water-dipping objective, and a DualView setup for simultaneous detection of two emission light spectra. For image acquisition and analysis, the Olympus cell^R software was used. A PE-conjugated antibody to Ly6C (1 μg; eBioscience) was injected intravenously to detect adhesion of $Ly6C^+CX_3CR1^+$ classical monocytes. In each cremaster, five fields of view were recorded for 30 s, and the number of adherent cells and the rolling flux (rolling monocytes passing a perpendicular line placed across the observed vessel) from each field were quantified. To reduce the variability between mice, values obtained from each field of view were added and are expressed as absolute values. Rolling speed was quantified by tracking individual cells for 30 s. In each cremaster muscle, five randomly chosen cells were tracked.

Leukocyte-endothelial interactions along the carotid artery were analyzed in $Apoe^{-/-}Cx_3cr1^{egfp/wt}$ mice that received high-fat diet for 4 weeks. Mice were placed in supine position, and the right jugular vein was cannulated with a catheter for peptide and antibody injection. The left external carotid artery was surgically exposed as described previously (*16*). Intravital microscopy was performed after injection of a PE-conjugated antibody to Ly6C (1 μg; eBioscience) using an Olympus BX51 microscope equipped with a Hamamatsu 9100-02 EMCCD camera, a DualView setup, and a 10× saline-immersion objective. Movies of 30 s were acquired and analyzed offline. In the carotid artery, one field of view was analyzed per mouse.

Statistics

All data are expressed as means ± SD. Because of variability between blood donors, data from flow adhesion assays are expressed as percent of control. Statistical calculations were performed using GraphPad Prism 5 (GraphPad Software Inc.). After calculating for normality by D'Agostino-Pearson omnibus test, Kruskal-Wallis test with post hoc Dunn's test, Mann-Whitney test, or paired *t* test was used. *P* values <0.05 were considered significant. Statistical tests and *P* values are specified for each panel in the respective figure legends. *n* indicated in the figure legends refers to biological replicates for in vitro assays and to the number of individual animals for in vivo observations.

SUPPLEMENTARY MATERIALS

www.sciencetranslationalmedicine.org/cgi/content/full/7/317/317ra196/DC1

Methods

Fig. S1. Secretory products of neutrophils and platelets do not affect adhesion of nonclassical monocytes.

Fig. S2. HNP1 and CCL5 stimulate classical monocyte adhesion via CCR5.

Fig. S3. CCL5 enables HNP1 to access CCR5.
Fig. S4. Design of an HNP1-CCL5 disrupting peptide.
Fig. S5. SKY peptide does not affect cell viability.
Fig. S6. SKY peptide dose-dependently reduces HNP1-CCL5–mediated monocyte adhesion.
Fig. S7. SKY peptide is nonfunctional in the absence of HNP1 and CCL5.
Fig. S8. SKY peptide is stable and exerts a long-lasting effect.
Fig. S9. SKY peptide inhibits HNP1-CCL5–evoked monocyte adhesion in large arteries.
Fig. S10. Presence of neutrophils and platelets after ischemia-reperfusion.
Fig. S11. HNP1, CCL5, and the SKY peptide do not affect monocyte homeostasis in myocardial ischemia-reperfusion injury.
Fig. S12. Purity of neutrophil and platelet preparations.
Table S1. CCL5-binding proteins as identified by mass spectrometry.
Table S2. Source data (Excel).
Movie S1. Summary of proposed mechanism.
Reference (*40*)

REFERENCES AND NOTES

1. J. W. Conlan, R. J. North, Neutrophils are essential for early anti-*Listeria* defense in the liver, but not in the spleen or peritoneal cavity, as revealed by a granulocyte-depleting monoclonal antibody. *J. Exp. Med.* **179**, 259–268 (1994).
2. A. Chalaris, B. Rabe, K. Paliga, H. Lange, T. Laskay, C. A. Fielding, S. A. Jones, S. Rose-John, J. Scheller, Apoptosis is a natural stimulus of IL6R shedding and contributes to the pro-inflammatory trans-signaling function of neutrophils. *Blood* **110**, 1748–1755 (2007).
3. O. Soehnlein, A. Zernecke, E. E. Eriksson, A. G. Rothfuchs, C. T. Pham, H. Herwald, K. Bidzhekov, M. E. Rottenberg, C. Weber, L. Lindbom, Neutrophil secretion products pave the way for inflammatory monocytes. *Blood* **112**, 1461–1471 (2008).
4. M. Drechsler, R. T. A. Megens, M. van Zandvoort, C. Weber, O. Soehnlein, Hyperlipidemia-triggered neutrophilia promotes early atherosclerosis. *Circulation* **122**, 1837–1845 (2010).
5. O. Soehnlein, L. Lindbom, C. Weber, Mechanisms underlying neutrophil-mediated monocyte recruitment. *Blood* **114**, 4613–4623 (2009).
6. P. A. Ward, Chemotaxis of mononuclear cells. *J. Exp. Med.* **128**, 1201–1221 (1968).
7. J. I. Gallin, M. P. Fletcher, B. E. Seligmann, S. Hoffstein, K. Cehrs, N. Mounessa, Human neutrophil-specific granule deficiency: A model to assess the role of neutrophil-specific granules in the evolution of the inflammatory response. *Blood* **59**, 1317–1329 (1982).
8. A. F. Gombart, H. P. Koeffler, Neutrophil specific granule deficiency and mutations in the gene encoding transcription factor C/EBPε. *Curr. Opin. Hematol.* **9**, 36–42 (2002).
9. O. Chertov, H. Ueda, L. L. Xu, K. Tani, W. J. Murphy, J. M. Wang, O. M. Z. Howard, T. J. Sayers, J. J. Oppenheim. Identification of human neutrophil-derived cathepsin G and azurocidin/CAP37 as chemoattractants for mononuclear cells and neutrophils. *J. Exp. Med.* **186**, 739–747 (1997).
10. M. C. Territo, T. Ganz, M. E. Selsted, R. Lehrer, Monocyte-chemotactic activity of defensins from human neutrophils. *J. Clin. Invest.* **84**, 2017–2020 (1989).
11. A. Vieira-de-Abreu, R. A. Campbell, A. S. Weyrich, G. A. Zimmerman, Platelets: Versatile effector cells in hemostasis, inflammation, and the immune continuum. *Semin. Immunopathol.* **34**, 5–30 (2012).
12. J. M. Burkhart M. Vaudel, S. Gambaryan, S. Radau, U. Walter, L. Martens, J. Geiger, A. Sickmann, R. P. Zahedi, The first comprehensive and quantitative analysis of human platelet protein composition allows the comparative analysis of structural and functional pathways. *Blood* **120**, e73–e82 (2012).
13. T. Baltus, P. von Hundelshausen, S. F. Mause, W. Buhre, R. Rossaint, C. Weber, Differential and additive effects of platelet-derived chemokines on monocyte arrest on inflamed endothelium under flow conditions. *J. Leukoc. Biol.* **78**, 435–441 (2005).
14. J. Bernhagen, R. Krohn, H. Lue, J. L. Gregory, A. Zernecke, R. R. Koenen, M. Dewor, I. Georgiev, A. Schober, L. Leng, T. Kooistra, G. Fingerle-Rowson, P. Ghezzi, R. Kleemann, S. R. McColl, R. Bucala, M. J. Hickey, C. Weber, MIF is a noncognate ligand of CXC chemokine receptors in inflammatory and atherogenic cell recruitment. *Nat. Med.* **13**, 587–596 (2007).
15. E. Karshovska, C. Weber, P. von Hundelshausen, Platelet chemokines in health and disease. *Thromb. Haemost.* **110**, 894–902 (2013).
16. O. Soehnlein, M. Drechsler, Y. Döring, D. Lievens, H. Hartwig, K. Kemmerich, A. Ortega-Gómez, M. Mandl, S. Vijayan, D. Projahn, C. D. Garlichs, R. R. Koenen, M. Hristov, E. Lutgens, A. Zernecke, C. Weber, Distinct functions of chemokine receptor axes in the atherogenic mobilization and recruitment of classical monocytes. *EMBO Mol. Med.* **5**, 471–481 (2013).
17. B. Passlick, D. Flieger, H. W. Ziegler-Heitbrock. Identification and characterization of a novel monocyte subpopulation in human peripheral blood. *Blood* **74**, 2527–2534 (1989).
18. F. Geissmann, S. Jung, D. R. Littman. Blood monocytes consist of two principal subsets with distinct migratory properties. *Immunity* **19**, 71–82 (2003).
19. C. Varol, A. Mildner, S. Jung. Macrophages: Development and tissue specialization. *Annu. Rev. Immunol.* **33**, 643–675 (2015).
20. C. Auffray, D. Fogg, M. Garfa, G. Elain, O. Join-Lambert, S. Kayal, S. Sarnacki, A. Cumano, G. Lauvau, F. Geissmann. Monitoring of blood vessels and tissues by a population of monocytes with patrolling behavior. *Science* **317**, 666–670 (2007).
21. D. Rittirsch, M. A. Flierl, P. A. Ward, Harmful molecular mechanisms in sepsis. *Nat. Rev. Immunol.* **8**, 776–787 (2008).
22. F. K. Swirski, M. Nahrendorf, Leukocyte behavior in atherosclerosis, myocardial infarction, and heart failure. *Science* **339**, 161–166 (2013).
23. S. Wantha, J.-E. Alard, R. T. A. Megens, A. M. van der Does, Y. Döring, M. Drechsler, C. T. N. Pham, M.-W. Wang, J.-M. Wang, R. L. Gallo, P. von Hundelshausen, L. Lindbom, T. Hackeng, C. Weber, O. Soehnlein, Neutrophil-derived cathelicidin promotes adhesion of classical monocytes. *Circ. Res.* **112**, 792–801 (2013).
24. P. B. Eisenhauer, R. I. Lehrer, Mouse neutrophils lack defensins. *Infect. Immun.* **60**, 3446–3447 (1992).
25. P. von Hundelshausen, K. S. C. Weber, Y. Huo, A. E. I. Proudfoot, P. J. Nelson, K. Ley, C. Weber, RANTES deposition by platelets triggers monocyte arrest on inflamed and atherosclerotic endothelium. *Circulation* **103**, 1772–1777 (2001).
26. O. Soehnlein, X. Xie, H. Ulbrich, E. Kenne, P. Rotzius, H. Flodgaard, E. E. Eriksson, L. Lindbom, Neutrophil-derived heparin-binding protein (HBP/CAP37) deposited on endothelium enhances monocyte arrest under flow conditions. *J. Immunol.* **174**, 6399–6405 (2005).
27. R. Chèvre, J. M. González-Granado, R. T. A. Megens, V. Sreeramkumar, C. Silvestre-Roig, P. Molina-Sánchez, C. Weber, O. Soehnlein, A. Hidalgo, V. Andrés. High-resolution imaging of intravascular atherogenic inflammation in live mice. *Circ. Res.* **114**, 770–779 (2014).
28. S. Epelman, P. P. Liu, D. L. Mann, Role of innate and adaptive immune mechanisms in cardiac injury and repair. *Nat. Rev. Immunol.* **15**, 117–129 (2015).
29. M. Nahrendorf, F. K. Swirski, E. Aikawa, L. Stangenberg, T. Wurdinger, J.-L. Figueiredo, P. Libby, R. Weissleder, M. J. Pittet. The healing myocardium sequentially mobilizes two monocyte subsets with divergent and complementary functions. *J. Exp. Med.* **204**, 3037–3047 (2007).
30. Y. Makino, D. N. Cook, O. Smithies, O. Y. Hwang, E. G. Neilson, L. A. Turka, H. Sato, A. D. Wells, T. M. Danoff, Impaired T cell function in RANTES-deficient mice. *Clin. Immunol.* **102**, 302–309 (2002).
31. J. W. Tyner, O. Uchida, N. Kajiwara, E. Y. Kim, A. C. Patel, M. P. O'Sullivan, M. J. Walter, R. A. Schwendener, D. N. Cook, T. M. Danoff, M. J. Holtzman, CCL5-CCR5 interaction provides antiapoptotic signals for macrophage survival during viral infection. *Nat. Med.* **11**, 1180–1187 (2005).
32. L. N. Sørensen, S. R. Paludan, Blocking CC chemokine receptor (CCR) 1 and CCR5 during herpes simplex virus type 2 infection in vivo impairs host defence and perturbs the cytokine response. *Scand. J. Immunol.* **59**, 321–333 (2004).
33. H.-J. Anders, M. Frink, Y. Linde, B. Banas, M. Wörnle, C. D. Cohen, V. Vielhauer, P. J. Nelson, H.-J. Gröne, D. Schlöndorff, CC chemokine ligand 5/RANTES chemokine antagonists aggravate glomerulonephritis despite reduction of glomerular leukocyte infiltration. *J. Immunol.* **170**, 5658–5666 (2003).
34. P. E. Westerweel, T. J. Rabelink, M. B. Rookmaaker, H.-J. Gröne, M. C. Verhaar, RANTES is required for ischaemia-induced angiogenesis, which may hamper RANTES-targeted anti-atherosclerotic therapy. *Thromb. Haemost.* **99**, 794–795 (2008).
35. C. Weber, K. S. C. Weber, C. Klier, S. Gu, R. Wank, R. Horuk, P. J. Nelson, Specialized roles of the chemokine receptors CCR1 and CCR5 in the recruitment of monocytes and T_H1-like/$CD45RO^+$ T cells. *Blood* **97**, 1144–1146 (2001).
36. T. Baltus, K. S. C. Weber, Z. Johnson, A. E. I. Proudfoot, C. Weber, Oligomerization of RANTES is required for CCR1-mediated arrest but not CCR5-mediated transmigration of leukocytes on inflamed endothelium. *Blood* **102**, 1985–1988 (2003).
37. P. von Hundelshausen, R. R. Koenen, M. Sack, S. F. Mause, W. Adriaens, A. E. I. Proudfoot, T. M. Hackeng, C. Weber, Heterophilic interactions of platelet factor 4 and RANTES promote monocyte arrest on endothelium. *Blood* **105**, 924–930 (2005).
38. M. Schiraldi, A. Raucci, L. M. Muñoz, E. Livoti, B. Celona, E. Venereau, T. Apuzzo, F. De Marchis, M. Pedotti, A. Bachi, M. Thelen, L. Varani, M. Mellado, A. Proudfoot, M. E. Bianchi, M. Uguccioni, HMGB1 promotes recruitment of inflammatory cells to damaged tissues by forming a complex with CXCL12 and signaling via CXCR4. *J. Exp. Med.* **209**, 551–563 (2012).
39. K. Wichapong, A. Rohe, C. Platzer, I. Slynko, F. Erdmann, M. Schmidt, W. Sippl, Application of docking and QM/MM-GBSA rescoring to screen for novel Myt1 kinase inhibitors. *J. Chem. Inf. Model.* **54**, 881–893 (2014).
40. C. Blanpain, V. Wittamer, J.-M. Vanderwinden, A. Boom, B. Renneboog, B. Lee, E. Le Poul, L. El Asmar, C. Govaerts, G. Vassart, R. W. Doms, M. Parmentier, Palmitoylation of CCR5 is critical for receptor trafficking and efficient activation of intracellular signaling pathways. *J. Biol. Chem.* **276**, 23795–23804 (2001).

Acknowledgments: We thank J. Brauner and R. Schrijver for excellent technical assistance. CCR5-GFP CHO cells were provided by J.-Y. Springael (Université Libre de Bruxelles, Belgium). **Funding:** O.S. received funding from the German Research Foundation (DFG) (SO876/4-1, SO876/6-1, SFB914 B08, and SFB1123 A06 and B05), the Else Kröner Fresenius Stiftung, and the Netherlands Organisation for Scientific Research (NWO) (VIDI project 91712303). J.-E.A. is a recipient of a postdoctoral scholarship from the Alexander von Humboldt Foundation. This work was supported by grants from Cyttron II (FES0908 to G.A.F.N. and T.M.H.) and by the Cardiovascular

Research Institute Maastricht. C.W. is funded by the European Research Council (ERC AdG 249929). C.S. is funded by the ERC (CIRCODE) and the DFG (Emmy-Noether SCHE1645/2-1 and SFB914 project B09). G.A.F.N. is supported by the NWO (Medium Investment Grant 91112016). R.M. receives funding from the DFG (INST 409/150-1 FUGG and SFB1123 Z01). **Author contributions:** J.-E.A., A.O.-G., K.W., D.B., M.H., G.L., B.F., J.R., N.P., J.N., H.I., D.S., X.B., F.G., and C.S. performed and analyzed the experiments; R.T.A.M., R.H., M.D., P.v.H., A.Z., T.M.H., and S.S. contributed to supervision and data analysis, and provided intellectual input; C.K., G.A.F.N., and C.W. contributed to study design, manuscript writing, data analyses, and funding; O.S. designed the study, wrote the manuscript, provided funding, performed experiments, and ran statistical analyses. **Competing interests:** The authors declare that they have no competing interests.

10.1126/scitranslmed.aad5330

Citation: J.-E. Alard, A. Ortega-Gomez, K. Wichapong, D. Bongiovanni, M. Horckmans, R. T. A. Megens, G. Leoni, B. Ferraro, J. Rossaint, N. Paulin, J. Ng, H. Ippel, D. Suylen, R. Hinkel, X. Blanchet, F. Gaillard, M. D'Amico, P. von Hundelshausen, A. Zarbock, C. Scheiermann, T. M. Hackeng, S. Steffens, C. Kupatt, G. A. F. Nicolaes, C. Weber, O. Soehnlein, Recruitment of classical monocytes can be inhibited by disturbing heteromers of neutrophil HNP1 and platelet CCL5. *Sci. Transl. Med.* **7**, 317ra196 (2015).